

**Bose-Einstein momentum correlations at fixed multiplicities:
Lessons from an exactly solvable thermal model for pp collisions
at the LHC**

M.D. Adzhymambetov¹, S.V. Akkelin¹, and Yu.M. Sinyukov¹

¹*Bogolyubov Institute for Theoretical Physics,
Metrolohichna 14b, 03143 Kyiv, Ukraine*

Abstract

Two-particle momentum correlations of N identical bosons are studied in the quantum canonical ensemble. We define the latter as properly selected sub-ensemble of events associated with the grand canonical ensemble which is characterized by a constant temperature and a harmonic-trap chemical potential. The merits of this toy-model are that it can be solved exactly, and that it demonstrates some interesting features revealed recently in small systems created in $p + p$ collisions at the LHC. We find that partial coherence can be observed in particles emission from completely thermal ensemble of events if instead of inclusive measurements one studies the two-boson distribution functions related to the events with particle numbers selected in some fixed multiplicity bins. The corresponding coherence effects increase with the multiplicity.

I. INTRODUCTION

Results from femtoscopic studies of two-particle momentum correlations (see e.g. Ref. [1]) from $p + p$ collisions at the CERN Large Hadron Collider (LHC) have been presented recently by the ALICE [2], ATLAS [3], CMS [4], and LHCb [5] Collaborations. It was found that the femtoscopic radii measured by the ATLAS and CMS Collaborations decrease with increasing momentum of a pair. It can be interpreted in hydrodynamical approach as the decrease of “lengths of homogeneity” [6] (sizes of the effective emission region) due to generated by hydrodynamical flow $x - p$ correlations. Also, one found that the “correlation strength” parameter λ is essentially less than unity. This is at variance with the expected behaviour for emission from thermalized systems [1]. Very interesting is also saturation effect in the multiplicity dependence of the interferometry correlation radius parameters for very high charged-particle multiplicity which was observed recently by the ATLAS [3] and CMS [4] Collaborations. Then while there is some evidence that hydrodynamics can be successfully applied to describe particle momentum spectra in high-multiplicity $p + p$ collisions (for recent review see e.g. Ref. [7]), it is still unclear whether the reported results on Bose-Einstein momentum correlations can be attributed to hydrodynamic evolution like in $A + A$ collisions.

In our opinion, observed peculiarities of Bose-Einstein momentum correlations in high-multiplicity $p + p$ collisions do not indicate inapplicability of hydrodynamics but can be partly associated with quantum coherence effects in small systems, when the effective system size is comparable with typical wavelength of the thermal bosons. Remind, that effective geometrical size is associated with length of homogeneity in the system [6]. The detail analysis of inclusive spectra and Bose-Einstein correlations in small thermal quantum systems was done very recently in Ref. [8]. It is shown that non-trivial coherence parameter appears in inclusive two-boson spectra only in the case of coherent condensate formation. On the other hand, in Ref. [9] the coherence effects in Bose-Einstein correlation functions in thermal systems are attributed to sub-ensembles of events with fixed multiplicities. It was found of suppressing the correlation functions in a finite canonical system in a large volume and low particle number density approximation. In the present paper, we study two-boson momentum correlations in small systems with high particle number densities at the moment of system break-up. It seems to be the case in high-multiplicity $p + p$ collisions at the LHC

where measured by the correlation femtoscopy method effective size of the system is near 1 fm. To make the problem tractable we utilize a model of the finite non-expanding system with smooth edges to avoid strong boundary effects. Keeping in mind the collective expansion inherent to systems created in particle and nucleus collisions, one can associate the corresponding system scale-parameter with the homogeneity length. We assume sharp particle momentum spectra freeze-out [10] immediately after emission, that is a reasonable approximation for $p + p$ collisions. In order to keep things as simple as possible, we consider non-relativistic ideal gas of bosons at fixed temperature trapped by a harmonic chemical potential. Such an exactly solvable toy-model of inhomogeneous and finite-sized systems is mathematically identical to an ideal bosonic gas trapped by a harmonic potential. Then we apply the fixed particle number constraint to the corresponding grand-canonical statistical operator and discuss influence of such constraints on one-particle momentum spectra and two-boson momentum correlations.

II. IDEAL GAS OF BOSONS IN A HARMONIC TRAP WITH FIXED PARTICLE NUMBER CONSTRAINT

We begin with a brief overview of the properties of the grand-canonical ensemble of non-interacting non-relativistic quantum-field bosons at fixed temperature, T , trapped by a harmonic chemical potential. For such a quantum field the Hamiltonian is given by

$$H = \int d^3r \Psi^\dagger(\mathbf{r}) \left(-\frac{1}{2m} \nabla^2 \right) \Psi(\mathbf{r}), \quad (1)$$

where the operators $\Psi^\dagger(\mathbf{r})$ and $\Psi(\mathbf{r})$ are the creation and annihilation operators, respectively. They fulfill the commutation relations

$$[\Psi(\mathbf{r}), \Psi^\dagger(\mathbf{r}')] = \delta^{(3)}(\mathbf{r} - \mathbf{r}'), \quad (2)$$

and

$$[\Psi(\mathbf{r}), \Psi(\mathbf{r}')] = [\Psi^\dagger(\mathbf{r}), \Psi^\dagger(\mathbf{r}')] = 0. \quad (3)$$

The Fourier transformed operators are defined as

$$\Psi(\mathbf{p}) = (2\pi)^{-3/2} \int d^3r e^{-i\mathbf{p}\mathbf{r}} \Psi(\mathbf{r}), \quad (4)$$

$$\Psi^\dagger(\mathbf{p}) = (2\pi)^{-3/2} \int d^3r e^{i\mathbf{p}\mathbf{r}} \Psi^\dagger(\mathbf{r}). \quad (5)$$

They satisfy the following canonical commutation relations:

$$[\Psi(\mathbf{p}), \Psi^\dagger(\mathbf{p}')] = \delta^{(3)}(\mathbf{p} - \mathbf{p}'), \quad (6)$$

and

$$[\Psi(\mathbf{p}), \Psi(\mathbf{p}')] = [\Psi^\dagger(\mathbf{p}), \Psi^\dagger(\mathbf{p}')] = 0. \quad (7)$$

The grand-canonical ensemble of such a system can be represented by the thermal statistical operator ρ ,

$$\rho = \frac{1}{Z} \hat{\rho}, \quad (8)$$

where Z is the grand-canonical partition function,

$$Z = Tr[\hat{\rho}], \quad (9)$$

and

$$\hat{\rho} = e^{-\beta \hat{H}}, \quad (10)$$

$$\hat{H} = \int d^3r \Psi^\dagger(\mathbf{r}) \left(-\frac{1}{2m} \nabla^2 - \mu(\mathbf{r}) \right) \Psi(\mathbf{r}), \quad (11)$$

where $\beta = 1/T$ is inverse temperature. The chemical potential, $\mu(\mathbf{r})$, reads

$$\mu(\mathbf{r}) = -\frac{m}{2}(\omega_x^2 x^2 + \omega_y^2 y^2 + \omega_z^2 z^2) + \hat{\mu}, \quad (12)$$

where $\hat{\mu} = \text{const.}$ The expectation value of an operator O can be expressed as

$$\langle O \rangle = Tr[\rho O]. \quad (13)$$

It is well known that \hat{H} is not diagonal in momentum (plane-wave) representation but can be diagonalized in the oscillator representation. Decomposing $\Psi(\mathbf{r})$ and $\Psi^\dagger(\mathbf{r})$ in terms of the harmonic oscillator eigenfunctions we get

$$\Psi(\mathbf{r}) = \sum_{n,k,l=0}^{\infty} \alpha(n, k, l) \phi_n(x) \phi_k(y) \phi_l(z), \quad (14)$$

where the creation, $\alpha^\dagger(n, k, l)$, and annihilation, $\alpha(n, k, l)$, operators satisfy the commutation relations

$$[\alpha(n, k, l), \alpha^\dagger(n', k', l')] = \delta_{nn'} \delta_{kk'} \delta_{ll'}, \quad (15)$$

and

$$[\alpha(n, k, l), \alpha(n', k', l')] = [\alpha^\dagger(n, k, l), \alpha^\dagger(n', k', l')] = 0. \quad (16)$$

Functions $\phi_n(x)$, $\phi_k(y)$, $\phi_l(z)$ are the harmonic oscillator eigenfunctions satisfying corresponding equations, e.g.

$$\left(\frac{d^2}{dx^2} - m\omega_x^2 x^2 + 2m\epsilon_n \right) \phi_n(x) = 0. \quad (17)$$

The normalized solution of Eq. (17) reads

$$\phi_n(x) = (2^n n! \pi^{1/2} b_x)^{-1/2} H_n \left(\frac{x}{b_x} \right) \exp \left(-\frac{1}{2} \left(\frac{x}{b_x} \right)^2 \right), \quad (18)$$

where $H_n(x/b_x)$ is the Hermite polynomial, and

$$\epsilon_n = \omega_x \left(n + \frac{1}{2} \right), \quad (19)$$

$$b_x = (m\omega_x)^{-1/2}. \quad (20)$$

Eigenfunctions (18) are complete,

$$\sum_{n=0}^{\infty} \phi_n(x) \phi_n^*(x') = \delta(x - x'), \quad (21)$$

and orthonormal

$$\int_{-\infty}^{\infty} \phi_n(x) \phi_{n'}^*(x) dx = \delta_{nn'}. \quad (22)$$

Then from Eq. (14) immediately follows that

$$\alpha(n, k, l) = \int_{-\infty}^{\infty} dx dy dz \phi_n^*(x) \phi_k^*(y) \phi_l^*(z) \Psi(\mathbf{r}). \quad (23)$$

In such a basis the \hat{H} reads

$$\hat{H} = \sum_{n,k,l=0}^{\infty} (\epsilon_n + \epsilon_k + \epsilon_l - \hat{\mu}) \alpha^\dagger(n, k, l) \alpha(n, k, l). \quad (24)$$

Equation (24) allows one to calculate expectation values (13) for products of α^\dagger and α operators. It can be done in various ways. It is more appropriate here to use the method which was used to prove the Wick's theorem for the grand-canonical ensemble, see e.g. Ref.

[11], as the extension of it can be used for the case of the canonical ensemble. First, using the eigenstates¹

$$|\mathbf{j}_1, \dots, \mathbf{j}_N\rangle = \frac{1}{\sqrt{N!}} \alpha^\dagger(\mathbf{j}_1) \dots \alpha^\dagger(\mathbf{j}_N) |0\rangle \quad (25)$$

of the particle number operator $\sum_{\mathbf{j}} \alpha^\dagger(\mathbf{j}) \alpha(\mathbf{j})$, and the identity

$$\sum_{N=0}^{\infty} \sum_{\mathbf{j}_1=\mathbf{0}}^{\infty} \dots \sum_{\mathbf{j}_N=\mathbf{0}}^{\infty} |\mathbf{j}_1, \dots, \mathbf{j}_N\rangle \langle \mathbf{j}_1, \dots, \mathbf{j}_N| = 1, \quad (26)$$

which express the completeness and normalization of this basis, one can insert Eq. (24) into Eq. (10) and write $\hat{\rho}$ in the harmonic oscillator basis,

$$\hat{\rho} = \sum_N \sum_{\mathbf{j}_1} \dots \sum_{\mathbf{j}_N} e^{-\beta(\epsilon_{\mathbf{j}_1} - \hat{\mu})} \dots e^{-\beta(\epsilon_{\mathbf{j}_N} - \hat{\mu})} |\mathbf{j}_1, \dots, \mathbf{j}_N\rangle \langle \mathbf{j}_1, \dots, \mathbf{j}_N|. \quad (27)$$

We denote here

$$\epsilon_{\mathbf{j}} = \epsilon_{n,k,l} = \epsilon_n + \epsilon_k + \epsilon_l = \omega_x \left(n + \frac{1}{2} \right) + \omega_y \left(k + \frac{1}{2} \right) + \omega_z \left(l + \frac{1}{2} \right). \quad (28)$$

Then, using an elementary operator algebra and Eq. (27) one can see that

$$\alpha(\mathbf{j}) \hat{\rho} = \hat{\rho} \alpha(\mathbf{j}) e^{-\beta(\epsilon_{\mathbf{j}} - \hat{\mu})}. \quad (29)$$

Using trace invariance under the cyclic permutation of an operator, we get

$$\begin{aligned} & Tr[\hat{\rho} \alpha^\dagger(\mathbf{j}_1) \alpha(\mathbf{j}_2)] = \\ & e^{-\beta(\epsilon_{\mathbf{j}_2} - \hat{\mu})} Tr[\hat{\rho} \alpha(\mathbf{j}_2) \alpha^\dagger(\mathbf{j}_1)] = e^{-\beta(\epsilon_{\mathbf{j}_2} - \hat{\mu})} (Tr[\hat{\rho} \alpha^\dagger(\mathbf{j}_1) \alpha(\mathbf{j}_2)] + \delta_{\mathbf{j}_1 \mathbf{j}_2} Tr[\hat{\rho}]). \end{aligned} \quad (30)$$

The Kronecker delta in the above equation, $\delta_{\mathbf{j}_1 \mathbf{j}_2}$, is

$$\delta_{\mathbf{j}_1 \mathbf{j}_2} = \delta_{n_1 n_2} \delta_{k_1 k_2} \delta_{l_1 l_2}. \quad (31)$$

From Eq. (30) we have

$$\langle \alpha^\dagger(\mathbf{j}_1) \alpha(\mathbf{j}_2) \rangle = \frac{1}{Tr[\hat{\rho}]} Tr[\hat{\rho} \alpha^\dagger(\mathbf{j}_1) \alpha(\mathbf{j}_2)] = \frac{\delta_{\mathbf{j}_1 \mathbf{j}_2}}{e^{\beta(\epsilon_{\mathbf{j}_2} - \hat{\mu})} - 1}, \quad (32)$$

which is a familiar Bose-Einstein distribution. It follows then that

$$\langle N \rangle = \sum_{\mathbf{j}} \langle \alpha^\dagger(\mathbf{j}) \alpha(\mathbf{j}) \rangle. \quad (33)$$

¹ For notational simplicity, here and below we write \mathbf{j} instead of (n, k, l) .

In a similar way, one can get

$$Tr[\hat{\rho}\alpha^\dagger(\mathbf{j}_1)\alpha^\dagger(\mathbf{j}_2)\alpha(\mathbf{j}_3)\alpha(\mathbf{j}_4)] = e^{-\beta(\epsilon_{\mathbf{j}_4}-\hat{\mu})}(\delta_{\mathbf{j}_1\mathbf{j}_4}Tr[\hat{\rho}\alpha^\dagger(\mathbf{j}_2)\alpha(\mathbf{j}_3)] + \delta_{\mathbf{j}_2\mathbf{j}_4}Tr[\hat{\rho}\alpha^\dagger(\mathbf{j}_1)\alpha(\mathbf{j}_3)] + Tr[\hat{\rho}\alpha^\dagger(\mathbf{j}_1)\alpha^\dagger(\mathbf{j}_2)\alpha(\mathbf{j}_3)\alpha(\mathbf{j}_4)]), \quad (34)$$

Then, taking into account Eq. (32) we have

$$\langle\alpha^\dagger(\mathbf{j}_1)\alpha^\dagger(\mathbf{j}_2)\alpha(\mathbf{j}_3)\alpha(\mathbf{j}_4)\rangle = \langle\alpha^\dagger(\mathbf{j}_2)\alpha(\mathbf{j}_3)\rangle\langle\alpha^\dagger(\mathbf{j}_1)\alpha(\mathbf{j}_4)\rangle + \langle\alpha^\dagger(\mathbf{j}_1)\alpha(\mathbf{j}_3)\rangle\langle\alpha^\dagger(\mathbf{j}_2)\alpha(\mathbf{j}_4)\rangle, \quad (35)$$

which is nothing but the particular case of the thermal Wick's theorem. Then, utilizing Eq. (14) and Eqs. (32) and (35) one can calculate expectation values of Ψ and Ψ^\dagger operators.

Now, let us apply the fixed particle number constraint to the grand-canonical statistical operator (8) to define canonical statistical operator ρ_N . For this aim, one can utilize the projection operator \mathcal{P}_N ,

$$\mathcal{P}_N = \frac{1}{N!} \int d^3r_1 \dots d^3r_N \Psi^\dagger(\mathbf{r}_1) \dots \Psi^\dagger(\mathbf{r}_N) |0\rangle \langle 0| \Psi(\mathbf{r}_1) \dots \Psi(\mathbf{r}_N), \quad (36)$$

which automatically invokes the corresponding constraint. Using Eqs. (14), (22) and (25) one can see that

$$\mathcal{P}_N = \sum_{\mathbf{j}_1} \dots \sum_{\mathbf{j}_N} |\mathbf{j}_1, \dots, \mathbf{j}_N\rangle \langle \mathbf{j}_1, \dots, \mathbf{j}_N|. \quad (37)$$

It is worth noting that such a projection is accompanied by the proper normalization in order to insure the probability interpretation of the ensemble obtained in result of this projection.

Then, using (37) we assert that the canonical statistical operator is

$$\rho_N = \frac{1}{Z_N} \hat{\rho}_N, \quad (38)$$

where

$$\hat{\rho}_N = \mathcal{P}_N \hat{\rho} \mathcal{P}_N = \sum_{\mathbf{j}_1} \dots \sum_{\mathbf{j}_N} e^{-\beta(\epsilon_{\mathbf{j}_1}-\hat{\mu})} \dots e^{-\beta(\epsilon_{\mathbf{j}_N}-\hat{\mu})} |\mathbf{j}_1, \dots, \mathbf{j}_N\rangle \langle \mathbf{j}_1, \dots, \mathbf{j}_N|, \quad (39)$$

and Z_N is the corresponding canonical partition function,

$$Z_N = Tr[\hat{\rho}_N]. \quad (40)$$

It follows from Eq. (39) that

$$Z = \sum_{N=0}^{\infty} Z_N. \quad (41)$$

The vacuum state, $N = 0$, yields $Z_0 = \langle 0|0 \rangle = 1$. Let us denote $\hat{\rho}_N$ associated with $\hat{\mu} = 0$ as $\hat{\rho}_N^0$. Then one can readily see that $\hat{\rho}_N = e^{\beta\hat{\mu}N} \hat{\rho}_N^0$ and

$$Z_N = e^{\beta\hat{\mu}N} Z_N^0. \quad (42)$$

Therefore, see Eq. (38), $e^{\beta\hat{\mu}N}$ is factored out and ρ_N does not depend on $\hat{\mu}$:

$$\rho_N = \frac{1}{Z_N^0} \hat{\rho}_N^0. \quad (43)$$

The expectation value of an operator O is defined as

$$\langle O \rangle_N = Tr[\rho_N O]. \quad (44)$$

It follows from Eqs. (39) and (44) that

$$\langle O \rangle = \sum_{N=0}^{\infty} \frac{Z_N}{Z} \langle O \rangle_N. \quad (45)$$

To evaluate the expectation values of operators $\alpha^\dagger(\mathbf{j}_1)\alpha(\mathbf{j}_2)$ and $\alpha^\dagger(\mathbf{j}_1)\alpha^\dagger(\mathbf{j}_2)\alpha(\mathbf{j}_3)\alpha(\mathbf{j}_4)$ with the canonical statistical operator ρ_N , one can adopt the procedure which was used above to calculate expectation values with the grand-canonical statistical operator ρ . It can be done in a similar way as it was done e.g. in Ref. [9]. For the reader's convenience, below we adjust the derivation from Ref. [9] for our model. A starting point is the relation

$$\alpha(\mathbf{j})\hat{\rho}_N^0 = \hat{\rho}_{N-1}^0 \alpha(\mathbf{j}) e^{-\beta\epsilon_{\mathbf{j}}} \quad (46)$$

which follows from Eq. (39) and commutation relations (15) and (16). Then one can exploit invariance under cyclic permutation and get the iteration equation

$$\langle \alpha^\dagger(\mathbf{j}_1)\alpha(\mathbf{j}_2) \rangle_N = e^{-\beta\epsilon_{\mathbf{j}_2}} \delta_{\mathbf{j}_1\mathbf{j}_2} \frac{Z_{N-1}^0}{Z_N^0} + e^{-\beta\epsilon_{\mathbf{j}_2}} \frac{Z_{N-1}^0}{Z_N^0} \langle \alpha^\dagger(\mathbf{j}_1)\alpha(\mathbf{j}_2) \rangle_{N-1}. \quad (47)$$

With the starting value $\langle \alpha^\dagger(\mathbf{j}_1)\alpha(\mathbf{j}_2) \rangle_0 = 0$ one can get from the above equation that

$$\langle \alpha^\dagger(\mathbf{j}_1)\alpha(\mathbf{j}_2) \rangle_N = \delta_{\mathbf{j}_1\mathbf{j}_2} \sum_{s=1}^N e^{-s\beta\epsilon_{\mathbf{j}_2}} \frac{Z_{N-s}^0}{Z_N^0}. \quad (48)$$

It follows from the definition of ρ_N , see Eqs. (38) and (39), that

$$\sum_{\mathbf{j}} \langle \alpha^\dagger(\mathbf{j}) \alpha(\mathbf{j}) \rangle_N = N. \quad (49)$$

Utilizing relation (46) we have

$$\langle \alpha^\dagger(\mathbf{j}_1) \alpha^\dagger(\mathbf{j}_2) \alpha(\mathbf{j}_3) \alpha(\mathbf{j}_4) \rangle_N = e^{-\beta \epsilon_{\mathbf{j}_4}} \frac{Z_{N-1}^0}{Z_N^0} \langle \alpha(\mathbf{j}_4) \alpha^\dagger(\mathbf{j}_1) \alpha^\dagger(\mathbf{j}_2) \alpha(\mathbf{j}_3) \rangle_{N-1}. \quad (50)$$

Then the same procedure leads to

$$\begin{aligned} \langle \alpha^\dagger(\mathbf{j}_1) \alpha^\dagger(\mathbf{j}_2) \alpha(\mathbf{j}_3) \alpha(\mathbf{j}_4) \rangle_N &= e^{-\beta \epsilon_{\mathbf{j}_4}} \frac{Z_{N-1}^0}{Z_N^0} \times \\ &(\langle \alpha^\dagger(\mathbf{j}_1) \alpha^\dagger(\mathbf{j}_2) \alpha(\mathbf{j}_3) \alpha(\mathbf{j}_4) \rangle_{N-1} + \delta_{\mathbf{j}_1 \mathbf{j}_4} \langle \alpha^\dagger(\mathbf{j}_2) \alpha(\mathbf{j}_3) \rangle_{N-1} + \delta_{\mathbf{j}_2 \mathbf{j}_4} \langle \alpha^\dagger(\mathbf{j}_1) \alpha(\mathbf{j}_3) \rangle_{N-1}). \end{aligned} \quad (51)$$

One can show by induction that Eq. (51) can be written as

$$\begin{aligned} \langle \alpha^\dagger(\mathbf{j}_1) \alpha^\dagger(\mathbf{j}_2) \alpha(\mathbf{j}_3) \alpha(\mathbf{j}_4) \rangle_N &= \\ \delta_{\mathbf{j}_1 \mathbf{j}_4} \sum_{s=1}^N e^{-s \beta \epsilon_{\mathbf{j}_4}} \frac{Z_{N-s}^0}{Z_N^0} \langle \alpha^\dagger(\mathbf{j}_2) \alpha(\mathbf{j}_3) \rangle_{N-s} &+ \delta_{\mathbf{j}_2 \mathbf{j}_4} \sum_{s=1}^N e^{-s \beta \epsilon_{\mathbf{j}_4}} \frac{Z_{N-s}^0}{Z_N^0} \langle \alpha^\dagger(\mathbf{j}_1) \alpha(\mathbf{j}_3) \rangle_{N-s}. \end{aligned} \quad (52)$$

Then, taking into account that $\langle \alpha^\dagger(\mathbf{j}_1) \alpha(\mathbf{j}_2) \rangle_0 = 0$ and Eq. (48), we get

$$\begin{aligned} \langle \alpha^\dagger(\mathbf{j}_1) \alpha^\dagger(\mathbf{j}_2) \alpha(\mathbf{j}_3) \alpha(\mathbf{j}_4) \rangle_N &= \\ (\delta_{\mathbf{j}_1 \mathbf{j}_4} \delta_{\mathbf{j}_2 \mathbf{j}_3} + \delta_{\mathbf{j}_1 \mathbf{j}_3} \delta_{\mathbf{j}_2 \mathbf{j}_4}) \sum_{s=1}^{N-1} \sum_{s'=1}^{N-s} e^{-s \beta \epsilon_{\mathbf{j}_4}} e^{-s' \beta \epsilon_{\mathbf{j}_3}} \frac{Z_{N-s-s'}^0}{Z_N^0}. \end{aligned} \quad (53)$$

The above expressions explicitly demonstrate deviations from the Wick's theorem in the canonical ensemble for a system of non-interacting bosons.

Canonical partition functions in Eqs. (48) and (53) can be calculated by means of the recursive formula of the canonical partition function for a system of N noninteracting bosons as given in Ref. [12] (an elementary derivation of it see e.g. in Ref. [9]):

$$n Z_n^0 = \sum_{s=1}^n \sum_{\mathbf{j}} e^{-s \beta \epsilon_{\mathbf{j}}} Z_{n-s}^0, \quad (54)$$

where $Z_0^0 = \langle 0|0 \rangle = 1$ and $n = 1, \dots, N$.

As a final comment we would like to point out that there is an essential difference between states defined by the grand-canonical statistical operator, ρ , see Eqs. (8), (9), (27), and canonical statistical operator, ρ_N , see Eqs. (38), (39), (40). While the former is mixture

of all N -particle states including vacuum state with $N = 0$, the latter is mixture of states with N fixed to some value. In a sense, quantum canonical state, ρ_N , can be interpreted as a state which is not completely chaotic but has some quantum coherent properties. In what follows we demonstrate that such a coherence is enhanced in the case of the Bose-Einstein condensation, when the number of particles in the ground state, N_0 , is of the order of the total number of particles, N ,² and discuss possible relations of our results to two-boson momentum correlations measured in $p + p$ collisions at the LHC.

III. PARTICLE MOMENTUM SPECTRA AND CORRELATIONS AT FIXED MULTIPLICITIES

In this Section we relate the model with physical observables in relativistic particle and nucleus collisions. To keep things as simple as possible, below we assume that $\omega_x = \omega_y = \omega_z \equiv \omega$. Note that mean particle number, $\langle N \rangle$, defined by the grand canonical ensemble, as well as particle number, N , in the canonical ensemble are the same for Ψ -particles and α -quasiparticles because unitary transformation (14) does not mix creation and annihilation operators.

First, let us estimate spatial size of the system at fixed multiplicities. It is defined as

$$\frac{1}{3}\sqrt{\langle \mathbf{r}^2 \rangle_N} = \langle x^2 \rangle_N = \frac{\int dx dy dz x^2 \langle \Psi^\dagger(\mathbf{r}) \Psi(\mathbf{r}) \rangle_N}{\int dx dy dz \langle \Psi^\dagger(\mathbf{r}) \Psi(\mathbf{r}) \rangle_N}, \quad (55)$$

where $\langle \Psi^\dagger(\mathbf{r}) \Psi(\mathbf{r}) \rangle_N$ is the mean particle number density in the canonical ensemble, and $\int dx dy dz \langle \Psi^\dagger(\mathbf{r}) \Psi(\mathbf{r}) \rangle_N = N$. From Eqs. (14) and (48) we get

$$\langle \Psi^\dagger(\mathbf{r}_1) \Psi(\mathbf{r}_2) \rangle_N = \sum_{s=1}^N \frac{Z_{N-s}^0}{Z_N^0} \sum_{n=0}^{\infty} \sum_{k=0}^{\infty} \sum_{l=0}^{\infty} \phi_n^*(x_1) \phi_k^*(y_1) \phi_l^*(z_1) \phi_n(x_2) \phi_k(y_2) \phi_l(z_2) e^{-\frac{3}{2}s\beta\omega} e^{-s\beta\omega(n+k+l)}, \quad (56)$$

where the eigenfunctions are defined by Eq. (18), $b_x = b_y = b_z \equiv b$ and

$$b = (m\omega)^{-1/2}, \quad (57)$$

see Eq. (20). Then, utilizing integral representation of the Hermite function (see e.g. Ref.

² This is definition of the Bose-Einstein condensation, see e.g. Ref. [13].

[14]),

$$H_n\left(\frac{x}{b}\right) = \left(\frac{b}{i}\right)^n \frac{b}{2\sqrt{\pi}} e^{\frac{x^2}{b^2}} \int_{-\infty}^{+\infty} v^n e^{-\frac{1}{4}b^2v^2 + ixv} dv, \quad (58)$$

one can perform summations over n, k, l in Eq. (56). A lengthy but straightforward calculation results in

$$\langle \Psi^\dagger(\mathbf{r}_1)\Psi(\mathbf{r}_2) \rangle_N = \sum_{s=1}^N \frac{1}{(2\pi)^{3/2}} \frac{1}{b^3} \frac{Z_{N-s}^0}{Z_N^0} (\sinh(\beta\omega s))^{-3/2} \exp\left(-\frac{\mathbf{r}_1^2 + \mathbf{r}_2^2}{2b^2 \tanh(\beta\omega s)}\right) \exp\left(\frac{\mathbf{r}_1\mathbf{r}_2}{b^2 \sinh(\beta\omega s)}\right). \quad (59)$$

Utilizing identity $(\tanh A)^{-1} - (\sinh A)^{-1} = \tanh(A/2)$, we have from Eq. (59) that mean particle number density in the canonical ensemble reads

$$\langle \Psi^\dagger(\mathbf{r})\Psi(\mathbf{r}) \rangle_N = \sum_{s=1}^N \frac{1}{(2\pi)^{3/2}} \frac{1}{b^3} \frac{Z_{N-s}^0}{Z_N^0} (\sinh(\beta\omega s))^{-3/2} \exp\left(-\frac{\tanh(\frac{1}{2}\beta\omega s)}{b^2} \mathbf{r}^2\right). \quad (60)$$

Substituting the above expression in Eq. (55) we readily find

$$\langle x^2 \rangle_N = \frac{1}{2} b^2 \frac{\sum_{s=1}^N \frac{Z_{N-s}^0}{Z_N^0} (\sinh(\beta\omega s))^{-3/2} (\tanh(\frac{1}{2}\beta\omega s))^{-5/2}}{\sum_{s=1}^N \frac{Z_{N-s}^0}{Z_N^0} (\sinh(\beta\omega s))^{-3/2} (\tanh(\frac{1}{2}\beta\omega s))^{-3/2}}. \quad (61)$$

To relate parameters of the model with physically meaningful parameters in relativistic particle and nucleus collisions, it is convenient to introduce parameter R such as

$$\omega = \frac{1}{R\sqrt{\beta m}}, \quad (62)$$

then $\frac{m\omega^2}{2} = \frac{1}{2\beta R^2}$, see Eq. (12). In what follows we treat R as free parameter instead of ω . As we will see below, R can be approximately associated with the spatial size of the system, $\langle x^2 \rangle_N$. Then

$$\beta\omega = \frac{1}{R} \sqrt{\frac{\beta}{m}} = \frac{\Lambda_T}{R}, \quad (63)$$

and

$$b = \frac{1}{\sqrt{m\omega}} = \sqrt{\Lambda_T R}, \quad (64)$$

where Λ_T is the thermal wave length, which we defined as

$$\Lambda_T = \frac{1}{\sqrt{mT}}. \quad (65)$$

We now turn to the two-particle momentum correlation functions. Two-particle momentum correlation function is defined as ratio of two-particle momentum spectrum to one-particle ones and can be written in canonical ensemble at fixed multiplicities as

$$C_N(\mathbf{k}, \mathbf{q}) = G_N \frac{\langle \Psi^\dagger(\mathbf{p}_1) \Psi^\dagger(\mathbf{p}_2) \Psi(\mathbf{p}_1) \Psi(\mathbf{p}_2) \rangle_N}{\langle \Psi^\dagger(\mathbf{p}_1) \Psi(\mathbf{p}_1) \rangle_N \langle \Psi^\dagger(\mathbf{p}_2) \Psi(\mathbf{p}_2) \rangle_N}. \quad (66)$$

Here $\mathbf{k} = (\mathbf{p}_1 + \mathbf{p}_2)/2$, $\mathbf{q} = \mathbf{p}_2 - \mathbf{p}_1$, and G_N is the normalization constant. The latter is needed to normalize the theoretical correlation function in accordance with normalization that is applied by experimentalists: $C^{exp}(\mathbf{k}, \mathbf{q}) \rightarrow 1$ for $|\mathbf{q}| \rightarrow \infty$.

Expressions in the denominator of Eq. (66) can be written immediately using Fourier transform of $\langle \Psi^\dagger(\mathbf{r}_1) \Psi(\mathbf{r}_2) \rangle_N$, see Eq. (59). We thus have

$$\langle \Psi^\dagger(\mathbf{p}_1) \Psi(\mathbf{p}_1) \rangle_N = \sum_{s=1}^N \frac{Z_{N-s}^0}{Z_N^0} \Phi_1(\mathbf{k}, \mathbf{q}, \beta\omega s), \quad (67)$$

$$\langle \Psi^\dagger(\mathbf{p}_2) \Psi(\mathbf{p}_2) \rangle_N = \sum_{s=1}^N \frac{Z_{N-s}^0}{Z_N^0} \Phi_1(\mathbf{k}, -\mathbf{q}, \beta\omega s), \quad (68)$$

where we introduced shorthand notation

$$\Phi_1(\mathbf{k}, \mathbf{q}, \beta\omega s) = \frac{b^3}{(2\pi \sinh(\beta\omega s))^{3/2}} \exp\left(-\left(\mathbf{k} - \frac{1}{2}\mathbf{q}\right)^2 b^2 \tanh\left(\frac{1}{2}\beta\omega s\right)\right). \quad (69)$$

Utilizing Eq. (53) and the same technique which was used to derive $\langle \Psi^\dagger(\mathbf{r}_1) \Psi(\mathbf{r}_2) \rangle_N$, we get after somewhat lengthy but straightforward calculations

$$\begin{aligned} & \langle \Psi^\dagger(\mathbf{p}_1) \Psi^\dagger(\mathbf{p}_2) \Psi(\mathbf{p}_1) \Psi(\mathbf{p}_2) \rangle_N = \\ & \sum_{s=1}^{N-1} \sum_{s'=1}^{N-s} \frac{Z_{N-s-s'}^0}{Z_N^0} (\Phi_1(\mathbf{k}, \mathbf{q}, \beta\omega s) \Phi_1(\mathbf{k}, -\mathbf{q}, \beta\omega s') + \Phi_2(\mathbf{k}, \mathbf{q}, s) \Phi_2(\mathbf{k}, -\mathbf{q}, \beta\omega s')), \end{aligned} \quad (70)$$

where we introduced notation

$$\Phi_2(\mathbf{k}, \mathbf{q}, \beta\omega s) = \frac{b^3}{(2\pi \sinh(\beta\omega s))^{3/2}} \exp\left(-\mathbf{k}^2 b^2 \tanh\left(\frac{1}{2}\beta\omega s\right) - \mathbf{q}^2 \frac{b^2}{4 \tanh\left(\frac{1}{2}\beta\omega s\right)}\right). \quad (71)$$

Inserting Eqs. (67), (68) and (70) in Eq. (66) gives us explicit expression for two-boson momentum correlation function at fixed multiplicities,

$$\begin{aligned} C_N(\mathbf{k}, \mathbf{q}) = G_N & \frac{\sum_{s=1}^{N-1} \sum_{s'=1}^{N-s} \frac{Z_{N-s-s'}^0}{Z_N^0} \Phi_1(\mathbf{k}, \mathbf{q}, \beta\omega s) \Phi_1(\mathbf{k}, -\mathbf{q}, \beta\omega s')}{\sum_{s=1}^N \frac{Z_{N-s}^0}{Z_N^0} \Phi_1(\mathbf{k}, \mathbf{q}, \beta\omega s) \sum_{s'=1}^N \frac{Z_{N-s'}^0}{Z_N^0} \Phi_1(\mathbf{k}, -\mathbf{q}, \beta\omega s')} + \\ & G_N \frac{\sum_{s=1}^{N-1} \sum_{s'=1}^{N-s} \frac{Z_{N-s-s'}^0}{Z_N^0} \Phi_2(\mathbf{k}, \mathbf{q}, s) \Phi_2(\mathbf{k}, -\mathbf{q}, \beta\omega s')}{\sum_{s=1}^N \frac{Z_{N-s}^0}{Z_N^0} \Phi_1(\mathbf{k}, \mathbf{q}, \beta\omega s) \sum_{s'=1}^N \frac{Z_{N-s'}^0}{Z_N^0} \Phi_1(\mathbf{k}, -\mathbf{q}, \beta\omega s')}. \end{aligned} \quad (72)$$

To estimate normalization constant G_N in Eq. (72), one needs utilize the limit $|\mathbf{q}| \rightarrow \infty$ at fixed \mathbf{k} in the corresponding expression. One can readily see that when $|\mathbf{q}| \rightarrow \infty$ at fixed \mathbf{k} then $C_N(\mathbf{k}, \mathbf{q}) \rightarrow G_N \frac{Z_{N-2}^0}{Z_N^0} \left(\frac{Z_N^0}{Z_{N-1}^0} \right)^2$. It follows then that proper normalization is reached if

$$G_N = \frac{Z_N^0}{Z_{N-2}^0} \left(\frac{Z_{N-1}^0}{Z_N^0} \right)^2. \quad (73)$$

IV. RESULTS AND DISCUSSION

In this Section, we calculate one-particle momentum spectra and two-particle Bose-Einstein momentum correlations in the model. For specificity, we assume that m is equal to pion mass and we take the set of parameters corresponding roughly to the values at the system's break-up in $p + p$ collisions at the LHC energies: The temperature T is set to 150 MeV, and for R we use 1.5 fm and 3 fm. The thermal wave length $\Lambda_T = 1/\sqrt{mT} \approx 1.36$ fm. We varied N in the range 1, ..., 20. Our aim here is to investigate how particle momentum spectra and correlations in the canonical ensemble with the fixed particle number constraint differ from the ones in the corresponding grand-canonical ensemble.

We start with calculations of the one-particle momentum spectra in the canonical ensemble, $n_N(\mathbf{p}) \equiv \langle \Psi^\dagger(\mathbf{p})\Psi(\mathbf{p}) \rangle_N$, see Eq. (67). We compare these calculations with the ones performed in the corresponding grand-canonical ensembles where $\hat{\mu}$ were found numerically to guarantee proper values of $\langle N \rangle$, such as $\langle N \rangle = N$. One-particle momentum spectra in the grand-canonical ensembles are calculated utilising Eq. (67) after substitution $\sum_{s=1}^N \frac{Z_{N-s}^0}{Z_N^0} \rightarrow \sum_{s=1}^{\infty} e^{\beta\hat{\mu}s}$. The results are plotted in Fig. 1 as a function of the particle momentum, for several different values of the radius parameter R and particle number N . Figure 1 demonstrates clearly that for used range of parameter values one-particle momentum spectra in the canonical ensembles can be approximated with good accuracy by the ones calculated in the corresponding grand-canonical ensembles.

Figure 2 displays two-boson momentum correlation functions (72) calculated in the canonical ensembles as a function of the momentum difference. From Fig. 2 it is evident that the intercept of the correlation function, $C_N(\mathbf{k}, \mathbf{0})$, is less than 2. This can be interpreted as a result of partial coherence of particles emission [1] because projection of the thermal grand-canonical ensemble into fixed- N subensemble results in the N -particle canonical state which is the state with partial coherence. Furthermore, one observes for small values of R

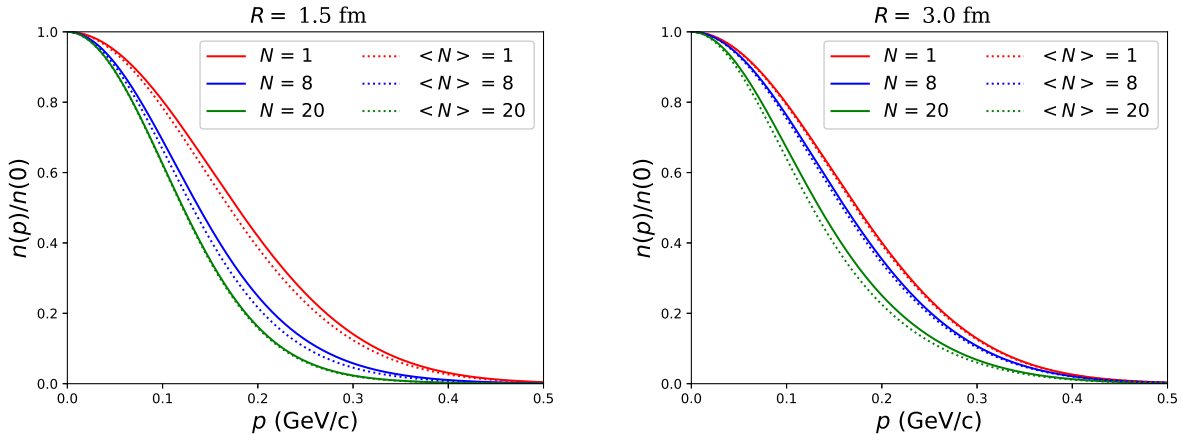


FIG. 1: Normalized $n(p_x, 0, 0)/n(\mathbf{0})$ momentum spectra calculated in the canonical ensembles with different N and R (solid lines), and corresponding spectra calculated in the grand-canonical ensembles with $\langle N \rangle = N$ (dotted lines).

essential non-Gaussianity of the correlation functions beyond the region of the correlation peak. It distinguishes two-boson correlation functions in the canonical ensembles from the ones in the corresponding grand-canonical ensembles where the correlation functions (not shown here) are well fitted by the Gaussian and intercept of the ones is equal to 2.

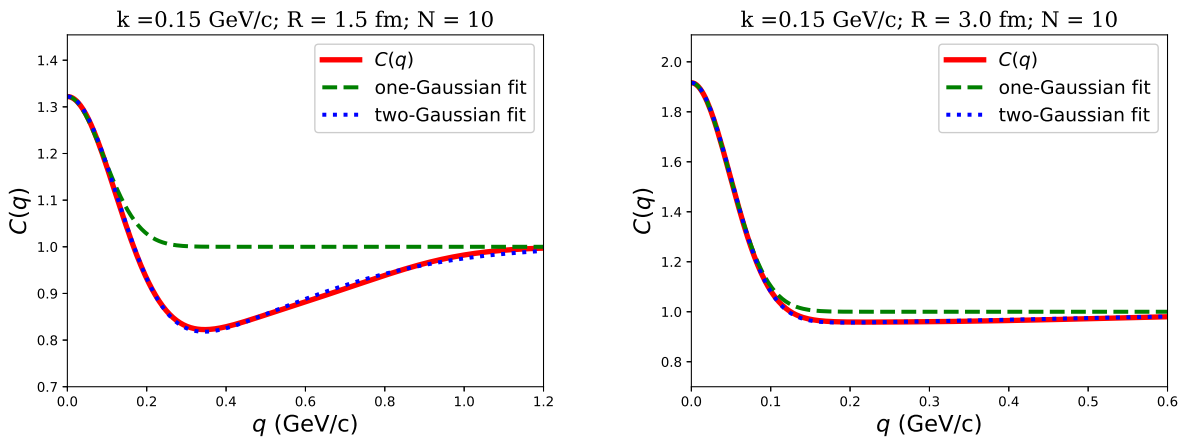


FIG. 2: Correlation functions (red solid lines) and their one- and two- Gaussian fits (blue dotted and green dashed lines, respectively) with $k = 0.15$ GeV/c, $N = 10$, $R = 1.5$ fm (left plot) and $R = 3.0$ fm (right plot). See text for details.

To analyze reasons for this behavior of the correlation functions in greater detail, let us first remark that correlation function $C_N(\mathbf{k}, \mathbf{q})$, see Eqs. (72), (73), can be parameterized

by the two-Gaussian expression

$$C_N^{2g}(\mathbf{k}, \mathbf{q}) = 1 - \lambda_1(\mathbf{k}, N)e^{-\mathbf{q}^2 R_1^2(\mathbf{k}, N)} + \lambda_2(\mathbf{k}, N)e^{-\mathbf{q}^2 R_2^2(\mathbf{k}, N)}, \quad (74)$$

where $\lambda_1 > 0$ and $\lambda_2 > 0$. Here $1 - \lambda_1(\mathbf{k}, N)e^{-\mathbf{q}^2 R_1^2(\mathbf{k}, N)}$ is associated with the first term in Eq. (72), and $\lambda_2(\mathbf{k}, N)e^{-\mathbf{q}^2 R_2^2(\mathbf{k}, N)}$ with the second one. The results of fittings are plotted in Fig. 2. It is evident that $C_N(\mathbf{k}, \mathbf{q})$ is rather well fitted by Eq. (74). This suggests that much of the non-Gaussian deviations observed in Fig. 2 arises from such a two-scale structure of the correlation function. If fitting procedure is restricted to the correlation peak region, then one observes from Fig. 2 that the correlation function is well fitted by the one-Gaussian expression

$$C_N^{1g}(\mathbf{k}, \mathbf{q}) = 1 + \lambda(\mathbf{k}, N)e^{-\mathbf{q}^2 R_{HBT}^2(\mathbf{k}, N)}, \quad (75)$$

where λ is equal to the intercept of the correlation function, $C_N(\mathbf{k}, \mathbf{0})$.

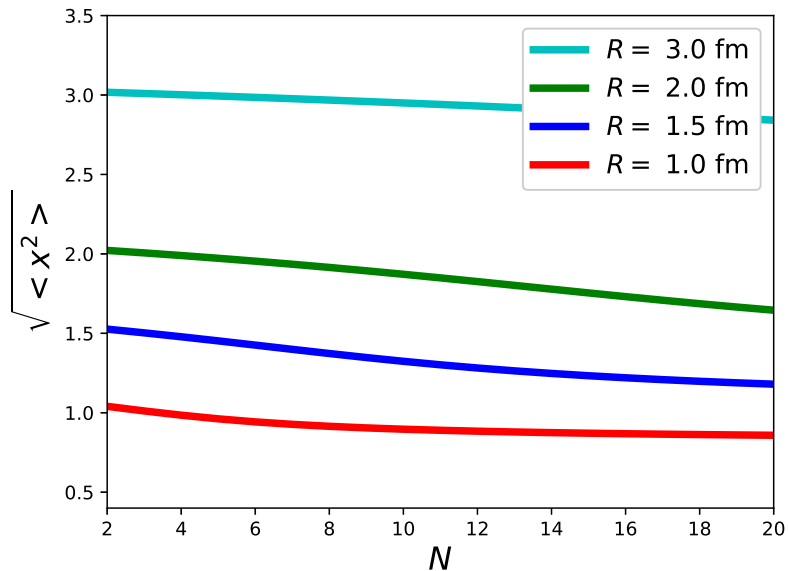


FIG. 3: The $\sqrt{\langle x^2 \rangle_N}$ dependence on N at different R .

From Fig. 2 it is clear that the value of the intercept of the correlation function is strongly dependent on the value of R at fixed N , namely, one observes that smaller values of R result in smaller values of the intercept of the correlation function. The question naturally arises: why decreasing the parameter R amounts to decreasing of the intercept? Some insight into this question may be gained from Fig. 3, in which mean size of the system, $\sqrt{\langle x^2 \rangle_N}$ (see

Eq. (61)), is plotted out to N . One observes from this Figure that parameter R roughly corresponds to the mean spatial size of the system in the varied range of N . It means that decrease of R at fixed N results in increase of the mean particle number density, $\propto N/R^3$.

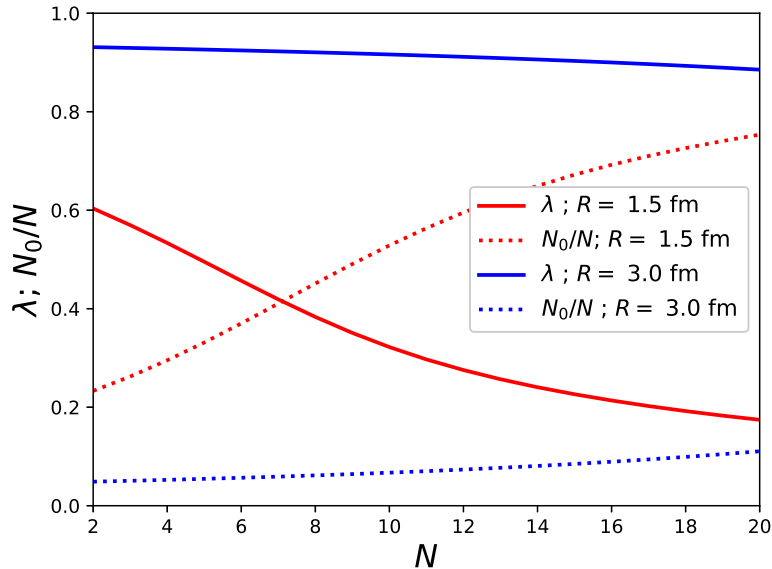


FIG. 4: The λ at $k = 0.15$ GeV/c, and N_0/N dependence on N for $R = 1.5$ fm and $R = 3.0$ fm.

To gain further insight into these results, the λ -parameter and the ratio of the ground-state population, $N_0 = \langle \alpha^\dagger(\mathbf{0})\alpha(\mathbf{0}) \rangle_N$ (see Eq. (48)), to the number of particles, N , are plotted out to N in Fig. 4. It can be seen from this Figure that the coherent effects, associated with the parameter λ , are significant for any N if the mean size of the system is comparable to or less than the thermal wave length Λ_T . One can also see from this Figure that increase of N results in increase of the value of N_0/N ratio and decrease of the value of λ -parameter. To interpret this result it is instructive to compare the canonical condensate fraction, N_0/N , with its grand-canonical counterpart $\langle N_0 \rangle / \langle N \rangle$. We start by noting that applying Cauchy's integral formula to Eqs. (41), (42) one can get (see, e.g., Ref. [15])

$$Z_N^0 = \beta \int_{\delta-i\infty}^{\delta+i\infty} \frac{d\hat{\mu}}{2\pi i} e^{-\hat{\mu}\beta N} Z(\hat{\mu}). \quad (76)$$

It is well known that utilizing the above expression for approximate evaluation of the canonical partition function, in the leading order of the saddle-point approximation one obtains

$$Z_N^0 \approx e^{-\hat{\mu}_\sigma \beta N} Z(\hat{\mu}_\sigma), \quad (77)$$

where $\hat{\mu}_\sigma$ is solution of the equation $\frac{d}{d\hat{\mu}}(-\hat{\mu}\beta N + \ln Z(\hat{\mu})) = 0$. For an ideal gas it means that $\hat{\mu}_\sigma$ is such that $\langle N \rangle = N$. Equation (77) becomes exact for $N \rightarrow \infty$. Then, using Eqs. (41), (42) and (45), one can expect that for finite but large N we get $N_0/N \approx \langle N_0 \rangle / \langle N \rangle$ where $\langle N_0 \rangle / \langle N \rangle$ is the condensate fraction in the grand-canonical ensemble with $\langle N \rangle = N$. Let us compare our results for the canonical condensate fraction, N_0/N , with the grand-canonical condensate fraction for a finite mean number of particles in a three-dimensional harmonic potential [16],

$$\frac{\langle N_0 \rangle}{\langle N \rangle} \approx 1 - \frac{\Delta}{\langle N \rangle (\beta\omega)^3}, \quad (78)$$

$$\Delta = \zeta(3) + \frac{3}{2}\zeta(2)\beta\omega, \quad (79)$$

calculated in the approximation $\beta\omega \ll 1$. Here $\zeta(x)$ is the Riemann zeta function, $\zeta(2) \approx 1.645$ and $\zeta(3) \approx 1.202$. In the above expression we have approximated $e^{\beta(\hat{\mu} - (3/2)\omega)} \approx 1$. Identifying $\langle N \rangle$ with the actual particle number N , and $\beta\omega$ with Λ_T/R , see Eq. (63), we compare N_0/N with $\langle N_0 \rangle / \langle N \rangle$ in Fig. 5 for $R = 1.5$ fm and $R = 3$ fm.

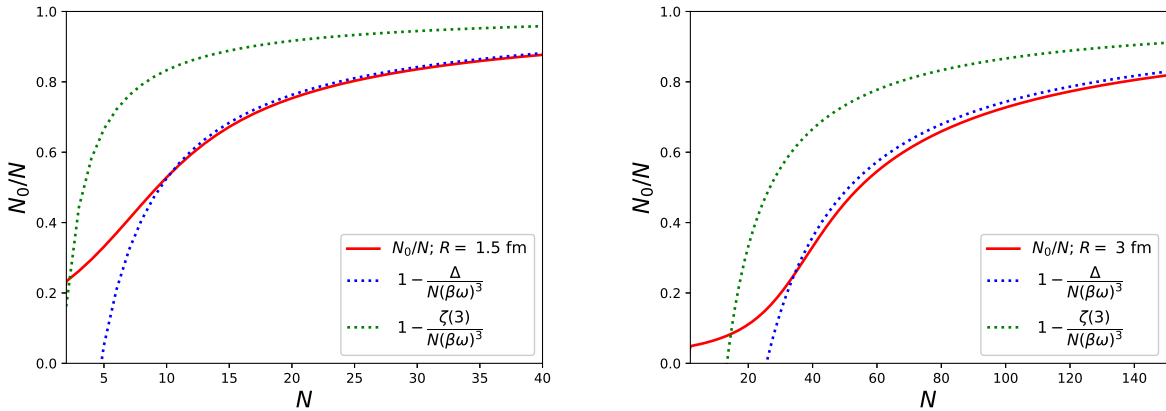


FIG. 5: Canonical N_0/N (red solid line) and its fits with Eq. (78) (blue and green dotted lines), $R = 1.5$ fm (left plot) and $R = 3.0$ fm (right plot). See text for details.

One observes that the approximate grand-canonical formula shows a rather good agreement with the exact canonical results even for not very large values of N . Loosely speaking, the canonical condensate fraction of the large system becomes noticeable (say, about 1/2) when the mean inter-particle distance, $(N/R^3)^{-1/3}$, becomes smaller than the correlation length, for an ideal gas the latter coincides with the thermal wave length, Λ_T .

While the quantitatively accurate description of the canonical condensate fraction within the grand-canonical approximation is manifest, it is not the case for fluctuations. It is well known that fluctuations in the ground state differ in the canonical and grand-canonical ensembles, and that for the latter the condensate fluctuations are very large, see e.g. Ref. [17] and references therein. In the canonical ensemble with a fixed number of particles such large fluctuations are impossible, and therefore increase of the ground-state fraction N_0/N increases “coherence” of the state. The latter distinguishes the ideal gas Bose-Einstein condensation in the canonical ensemble from the ideal gas Bose-Einstein condensation in the grand-canonical ensemble. It is well known that the intercept of the two-boson momentum correlation function for a maximally mixed (chaotic) state is equal to 2, and that the one for a pure state is equal to 1, see e.g. Ref. [1]. Therefore increase of the ground-state fraction, N_0/N , results in decreasing of the λ -parameter.

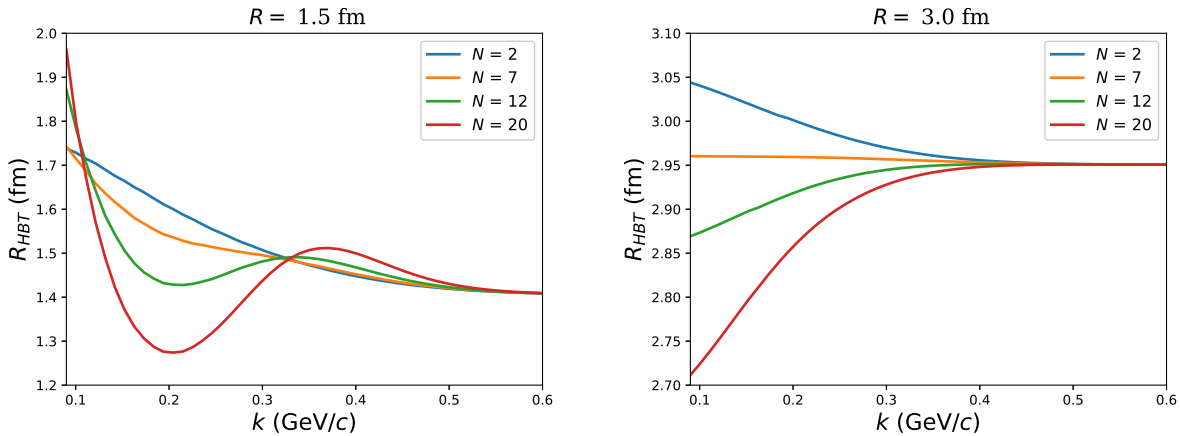


FIG. 6: HBT radii obtained from the one-Gaussian fit of the two-boson correlation function in the canonical ensembles with different N , as a function of the pair average momentum k .

Finally, in Fig. 6 we plot the R_{HBT} as a function of the pair momenta, k , for different R and N . One observes a consistent trend: by increasing k the interferometry radii, R_{HBT} , become independent on N .

V. CONCLUSIONS

Usually one does not care so much about quantum coherence in the canonical ensemble at fixed multiplicities.³ However, utilizing the simple analytically solvable model, we demonstrated that the formulas derived in the fixed- N canonical ensemble for a small inhomogeneous thermal system are not always accurately approximated by the grand-canonical ones with $\langle N \rangle = N$. Namely, we noticed that while the one-particle momentum spectra can be well approximated by the corresponding grand-canonical ensemble expressions, it is not the case for the two-boson momentum correlations. Interestingly, we observed that the most significant deviations arise if the particle number density in the canonical ensemble can increase with N . In the considered simple model it implies that interferometry radii are independent on N at moderately high pair momenta. Then for fairly high N the particle number density exceeds some limit value leading to the noticeable Bose-Einstein condensation in the corresponding ground state of the fixed- N canonical ensemble state. Such a condensation strengthens the coherence properties of the canonical ensemble state, and results in the decreasing of the intercept of the two-boson momentum correlation function when N increases. This may explain the observed phenomenon of partial quantum coherence in high-multiplicity $p + p$ collisions events in fixed multiplicity bins at the LHC energies [3, 4]. It would be very interesting to revisit the results of experimental studies in view of our findings.

The main lesson from this study is that the canonical and grand-canonical ensembles can yield different results for two-boson momentum correlations of particles emitted by small inhomogeneous systems. The results of our analysis can be useful to disentangle the effects on the shape of the measured correlation function which can be attributed to an experimental selection of events in fixed multiplicity bins from those which are due to thermalization and flow. Therefore, determination of the extent to which our results can be generalized for a realistic model of heavy ion and particle collisions could be of great interest.

³ See however Ref. [18] where it was demonstrated that description in hydrodynamic approach of the interferometry radii in $p + p$ collisions is improved if account for mutual quantum coherence of closely located emitters caused by the uncertainty principle.

Acknowledgments

The research was partially (M.A. and Yu.S.) carried out within NAS of Ukraine priority project “Fundamental properties of the matter in the relativistic collisions of nuclei and in the early Universe” (No. 0120U100935).

- [1] M. Gyulassy, S.K. Kauffmann, and L.W. Wilson, *Phys. Rev. C* **20**, 2267 (1979); M.I. Podgoretsky, *Fiz. Elem. Chast. At. Yad.* **20**, 628 (1989) [*Sov. J. Part. Nucl.* **20**, 266 (1989)]; D.H. Boal, C.-K. Gelbke, B.K. Jennings, *Rev. Mod. Phys.* **62**, 553 (1990); U.A. Wiedemann, U. Heinz, *Phys. Rep.* **319**, 145 (1999); R.M. Weiner, *Phys. Rep.* **327**, 249 (2000); R.M. Weiner, *Introduction to Bose-Einstein Correlations and Subatomic Interferometry* (Wiley, New York, 2000); M. Lisa, S. Pratt, R. Soltz, U. Wiedemann, *Annu. Rev. Nucl. Part. Sci.* **55**, 357 (2005); R. Lednický, *Phys. Part. Nuclei* **40**, 307 (2009) [arXiv:nucl-th/0501065]; Yu.M. Sinyukov, V.M. Shapoval, *Phys. Rev. D* **87**, 094024 (2013).
- [2] K. Aamodt *et al.* (ALICE Collaboration), *Phys. Rev. D* **84**, 112004 (2011); S. Acharya *et al.* (ALICE Collaboration), *J. High Energ. Phys.* **2019**, 108 (2019). [https://doi.org/10.1007/JHEP09\(2019\)108](https://doi.org/10.1007/JHEP09(2019)108)
- [3] ATLAS Collaboration, *Eur. Phys. J. C* **75**, 466 (2015).
- [4] A.M. Sirunyan *et al.* (CMS Collaboration), *Phys. Rev. C* **97**, 064912 (2018); *J. High Energ. Phys.* **2020**, 14 (2020). [https://doi.org/10.1007/JHEP03\(2020\)014](https://doi.org/10.1007/JHEP03(2020)014)
- [5] The LHCb Collaboration, *J. High Energ. Phys.* **2017**, 25 (2017). [https://doi.org/10.1007/JHEP12\(2017\)025](https://doi.org/10.1007/JHEP12(2017)025)
- [6] Yu.M. Sinyukov, *Nucl. Phys. A* **566**, 589c (1994); Yu.M. Sinyukov, in: *Hot Hadronic Matter: Theory and Experiment* edited by J. Letessier, H.H. Gutbrod, and J. Rafelski (Plenum, New York, 1995), p. 309; S.V. Akkelin, Yu.M. Sinyukov, *Phys. Lett. B* **356**, 525 (1995); S.V. Akkelin, Yu.M. Sinyukov, *Z. Phys. C* **72**, 501 (1996).
- [7] J.L. Nagle, W.A. Zajc, *Ann. Rev. Nucl. Part. Sci.* **68**, 211 (2018); C. Shen, arXiv:2001.11858.
- [8] M.D. Adzhymambetov, Yu.M. Sinyukov, *Phys. Rev. D* **102**, 036019 (2020).
- [9] S.V. Akkelin, Yu.M. Sinyukov, *Phys. Rev. C* **94**, 014908 (2016).
- [10] F. Cooper, G. Frye, *Phys. Rev. D* **10**, 186 (1974).

- [11] C. Bloch, C. De Dominicis, Nucl. Phys. **7**, 459 (1958); M. Gaudin, Nucl. Phys. **15**, 89 (1960); N.N. Bogolubov, N.N. Bogolubov, Jr., *An Introduction to Quantum Statistical Mechanics* (Gordon and Breach, New York, 1992); S.R. de Groot, W.A. van Leeuwen, Ch. G. van Weert, *Relativistic Kinetic Theory* (North-Holland, Amsterdam, 1980).
- [12] P.T. Landsberg, *Thermodynamics* (Interscience, New York, 1961); P. Borrmann and G. Franke, J. Chem. Phys. **98**, 2484 (1993).
- [13] A.J. Leggett, Rev. Mod. Phys. **73**, 307 (2001).
- [14] I.S. Gradshteyn, I.M. Ryzhik, *Table of Integrals, Series and Products* (Academic, New York, 1980).
- [15] K. Huang, *Statistical Mechanics* (John Wiley & Sons, New York, 1963); R.M. Ziff, G.E. Uhlenbeck, and M. Kac, Phys. Rep. **32**, 169 (1977).
- [16] W. Ketterle, N.J. van Druten, Phys. Rev. A **54**, 656 (1996).
- [17] Vitaly V. Kocharovsky, Vladimir V. Kocharovsky, Martin Holthaus, C.H. Raymond Ooi, Anatoly Svidzinsky, Wolfgang Ketterle, Marlan O. Scully, Advances In Atomic, Molecular, and Optical Physics **53**, 291 (2006).
- [18] V.M. Shapoval, P. Braun-Munzinger, Iu.A. Karpenko, Yu.M. Sinyukov, Phys. Lett. B **725**, 139 (2013).